SNS Storage Ring Impedances

BNL/SNS TECHNICAL NOTE

NO. 061

S. Y. Zhang

March 26, 1999

ALTERNATING GRADIENT SYNCHROTRON DEPARTMENT
BROOKHAVEN NATIONAL LABORATORY
UPTON, NEW YORK 11973

I. Introduction

The SNS storage ring impedance budget is presented in this article. The results are preliminary, further investigation of this matter is needed. The first reason is that the design of the ring is still in progress, and the second is that many impedance issues have to be settled by the measurement.

The impedances of a synchrotron fall in several categories, and they need to be treated differently.

1. Resonant modes of broad band impedance are in a few GHz. Therefore, below 1 GHz, this impedance can be seen as an inductance. The bellows, steps, ports, etc., contribute to the broad band impedance. The general relation between the longitudinal and transverse impedances, $Z_T \approx (Z_\ell/n)\, 2R/\beta b^2$, can be applied [1].

2. Resonant modes of low frequency impedance [2,3] are in a few tens to several hundred MHz. For relevant frequency range of up to 1 GHz, not only the imaginary part cannot be seen as a pure inductance, the real part of the impedance might not be negligible, also. There is no general relations between the longitudinal and transverse impedances. The low frequency impedance includes the BPM, the extraction and injection kickers.

3. Resistive wall impedance is of interest at very low frequency range. The relation of $Z_T \approx (Z_\ell/n)\, 2R/\beta b^2$ exits. Sometimes, one estimates the resistive wall impedance by its value at the revolution frequency.

4. Space charge impedance is frequency independent, and it is negative inductive. This impedance is a dominant one in the SNS storage ring.

5. Narrow band impedances are mainly from the RF cavities. However, parasitic parameter may cause sharp resonance in the kicker impedance, and large steps and cavities of the vacuum chamber may also be the sources of narrow band impedance.

II. Resistive Wall Impedance

Assuming a smooth cylindrical vacuum chamber, the longitudinal and transverse resistive wall impedances are,

$$Z_\ell(\omega) = (sgn(\omega) + j)\frac{\beta Z_0 \delta_s}{2b}\frac{\omega}{\omega_0} \tag{1}$$

and

$$Z_T(\omega) = (sgn(\omega) + j)\frac{R Z_0 \delta_s}{b^3} \tag{2}$$

where Z_0 is the impedance in free space, 377 Ω, b is the radius of the vacuum chamber and R is the machine radius. The skin depth at the frequency ω is defined as,

$$\delta_s = \sqrt{\frac{2\rho}{\mu_0|\omega|}} \tag{3}$$

where ρ is the resistivity of the vacuum chamber, for stainless steel it is $\rho = 0.73 \times 10^{-6}\ \Omega m$, and $\mu_0 = 4\pi \times 10^{-7}\ H/m$ is the permeability of free space.

For the SNS [4], $R = 35.1\ m$, and the average beam pipe radius is taken as $b = 10\ cm$. At the revolution frequency 1.189 MHz, we get $\delta_s = 0.39$ mm, and the longitudinal and transverse resistive wall impedances at the revolution frequency are

$$Z_\ell(\omega_0) = 0.65(1 + j)\Omega \tag{4}$$

and

$$Z_T(\omega_0) = 5.22(1 + j)K\Omega/m \tag{5}$$

respectively.

Since the fractional tune is 0.82, the most damaging resistive wall impedance is $Z_T(-0.18\omega_0) = (-1 + j)\ 12.31\ K\Omega/m$.

III. Space Charge Impedance

The longitudinal space charge impedance is defined as,

$$Z_\ell(\omega) = -j\frac{gZ_0}{2\beta\gamma^2}\frac{\omega}{\omega_0} \tag{6}$$

where

$$g = 1 + 2\ln\frac{b}{a} \tag{7}$$

For Gaussian distribution, $a = \sqrt{2}\sigma$, where σ is the transverse *rms* beam size.

The transverse space charge impedance is,

$$Z_T(\omega) = -j\frac{RZ_0}{\beta^2\gamma^2}(\frac{1}{a^2} - \frac{1}{b^2}) \tag{8}$$

For SNS, $\beta = 0.875$, $\gamma = 2.066$, taking $a = \sqrt{2}\sigma = 2.36\ cm$, then the longitudinal and transverse space charge impedances are

$$Z_\ell(\omega_0) = -j196\ \Omega \tag{9}$$

and

$$Z_T(\omega) = -j6.87\ M\Omega/m \tag{10}$$

respectively.

The longitudinal impedance can be written as Z_ℓ/n, with $n = \omega/\omega_0$. Thus, we have $Z_\ell/n = Z_\ell(\omega_0)$.

Both Z_ℓ/n and Z_T are independent of the frequency and appear to be negative inductive.

IV. Broad Band Impedance

The broad band impedance is caused by the bellows, steps, vacuum ports and valves. The impedance of the collimator can be seen as the combination of a resistive wall with smaller pipe radius, and the steps as well, but it is dominated by the steps. The models of these components will be presented, and the longitudinal impedance will be estimated. The transverse impedance will be obtained by using

$$Z_T \approx \frac{2R}{\beta b^2}\left(\frac{Z_\ell}{n}\right) \tag{11}$$

with $b = 10\ cm$. Since the real part of these impedance rises only above the pipe cut-off frequency, therefore, it is negligible. Only the imaginary part of the impedance will be presented.

A. Model

1. Pillbox

The impedance of bellows and steps can be estimated using a model of pillbox. In all cases, we assume the worst case without tapering at the transitions.

If the dimension of the discontinuity, i.e. width w and height h, of a pillbox are smaller than the pipe radius b, then for the low frequency, $\omega \ll 2.405c/b$, the impedance of the pillbox is reduced to two quasistatic problems, i.e. electrostatic and magnetostatic ones [5]. Assuming the beam azimuthal magnetic field fills up the pillbox, the oscillation of this flux with time generates a solenoidal electric field. The electric term to the impedance comes from the distortion of the beam potential field by the pipe discontinuity.

For the magnetic term, the longitudinal impedance is

$$Z_{\ell m} = j\omega \frac{Z_0 \alpha_m}{2\pi bc} \tag{12}$$

where α_m is the magnetic polarizability of the discontinuity. For small pillbox, $\alpha_m = S$, where S is the cross section of the enlargement.

For the electric term, the longitudinal impedance is

$$Z_{\ell e} = j\omega \frac{Z_0 \alpha_e}{4\pi bc} \tag{13}$$

where α_e is the electric polarizability of the discontinuity.

The function α_e has the asymptotic behavior,

$$\alpha_e = -\frac{w^2}{\pi}, \text{ if } g \leq h \tag{14}$$

and

$$\alpha_e = -2wh + \frac{2h^2}{\pi}\left(2\ln\frac{2\pi g}{h} + 1\right), \text{ if } w \gg h \tag{15}$$

Therefore, total impedance for short pillbox ($w \leq h$) is

$$Z_\ell = j\omega \frac{Z_0}{2\pi bc}\left(wh - \frac{w^2}{2\pi}\right) \tag{16}$$

which is inductive. The electric contribution is negative and small. In [6], this part is neglected.

For a deep pillbox, $h \sim b$, the magnetic polarizability of the discontinuity is $\alpha_m = wb\ln(1 + h/b)$, rather than $\alpha_m = wh$, which is valid if $h \ll b$. The electric term needs no corrections. Thus, the impedance is,

$$Z_\ell = j\omega \frac{Z_0}{2\pi bc}\left(wb\ln(1+\frac{h}{b}) - \frac{w^2}{2\pi}\right) \tag{17}$$

If $w \gg h$, we have

$$Z_\ell = j\omega \frac{Z_0 h^2}{2\pi^2 bc}\left(2\ln\frac{2\pi w}{h} + 1\right) \tag{18}$$

where $w < b$ is still required.

Increase further the length w beyond b, the situation becomes two separate steps. The transition is at $w = b$. Simply substitute w by b, and divide by 2 in the equation (18), we have

$$Z_\ell = j\omega \frac{Z_0 h^2}{4\pi^2 bc}\left(2\ln\frac{2\pi b}{h} + 1\right) \tag{19}$$

2. Iris

In the case of an iris, both magnetic and electric dipole moments change sign. However, the electric term is larger than the magnetic one, and the impedance is still inductive.

For $w \gg h$, the impedance is the same as the shallow cavity, i.e. equation (18) can be used.

For a thin iris, $w \ll h$, it becomes,

$$Z_\ell = j\omega \frac{Z_0}{4bc}\left(h^2 + \frac{wh}{\pi}\left(\ln\frac{8\pi w}{h} - 3\right)\right) \tag{20}$$

This equation is derived with $h \ll b$, where the verification was made using the simulations.

3. Ports

The longitudinal impedance associated with a round vacuum pumping hole of radius b_{port} can be estimated as [7],

$$\frac{Z_\ell}{n} = j\frac{Z_0}{6\pi^2}\frac{b_{port}^3}{Rb^2} \tag{21}$$

and the general relation between the longitudinal and transverse impedances, the equation (11), can be used.

B. Impedance of bellows

For the SNS, there are 40 bellows at $b = 10\ cm$, each has 20 corrugations with the period of 0.75 cm, i.e. $w = 3.75\ mm$, and the depth $h = 1.5\ cm$. Also, there are 32 bellows at $b = 15\ cm$, each has 10 corrugations with the period of 1.5 cm, i.e. $w = 7.5\ mm$, and the depth $h = 2\ cm$. Using the equation (16), we have

$$\frac{Z_\ell}{n} = j1.1\Omega \tag{22}$$

and

$$Z_T = j8.8\ K\Omega/m \tag{23}$$

C. Impedance of steps

The impedance of steps can be estimated by using the equation (19). Note that the difference between a step-up and a step-down is disregarded.

The normal vacuum chamber radius is $b = 10\ cm$. However, there are total 8 large quads with $b = 15\ cm$, which result in 16 steps from 10 cm to 15 cm. For the 40 BPM's associated with normal quads, there are 80 steps from 10 cm to 12 cm, and for 8 BPM's with large quads, there are 16 steps from 15 cm to 17 cm. The present design shows that half of BPM tanks' steps are with taper.

The average vertical radius for all dipoles is taken as 8 cm. Therefore, for 32 dipoles, there are 64 steps from 8 cm to 10 cm. Half of these steps are with a 3" taper, and another half is not decided yet.

Consider the horizontal steps. For 16 steps, with $b = 10\ cm$, $h = 15\ cm$, we have $Z_\ell/n = j3.3\Omega$. For 80 steps, with $b = 10\ cm$, $h = 12\ cm$, we

get $Z_\ell/n = j11.8\Omega$, and for 16 steps, with $b = 15\ cm$, $h = 17\ cm$, we have $Z_\ell/n = j3.2\Omega$. In total, we have, $Z_\ell/n = j18.3\Omega$.

There are additional 64 vertical steps, with $b = 8\ cm$, $h = 10\ cm$, which result in $Z_\ell/n = j8.0\Omega$.

It is shown in [8] that for LHC, a taper length about twice of the transition height helps to reduce both longitudinal and transverse impedances by a factor of 2. A further extension to 10 times of the transition height reduced the longitudinal impedance by another 25%, and the transverse, 40%. This is approximately agreeable to the results in [9].

Let us take the shielding effect of the striplines at a BMP tank as a factor of 2 reduction in impedance. Also we assume that half of the transitions at dipoles are with taper, resulted in the impedance reduction by a factor of 2. The total vertical step impedance is,

$$\frac{Z_\ell}{n} = j16.8\Omega \tag{24}$$

and

$$Z_T = j134.4\ K\Omega/m \tag{25}$$

The horizontal impedance is a little smaller than the vertical one, but both are much larger than the impedance caused by the bellows.

D. Impedance of ports

The storage ring has total 64 round vacuum pumping holes, with 6" diameter. We take $b_{port} = 7.5\ cm$. Let the beam pipe radius be $b = 10\ cm$, we get the total longitudinal impedance

$$\frac{Z_\ell}{n} = j0.49\ \Omega \tag{26}$$

and the transverse impedance

$$Z_T = j3.9\ K\Omega/m \tag{27}$$

E. Impedance of valves

There are 8 vacuum valves at $b = 10\ cm$, and we may also have 8 valves at $b = 12.5\ cm$. Let a valve be roughly described by a pillbox with $w = 5$

cm, and $h = 4\ cm$. Using the equation (17), we get the total longitudinal impedance

$$\frac{Z_\ell}{n} = j0.28\ \Omega \tag{28}$$

and the transverse impedance

$$Z_T = j2.2\ K\Omega/m \tag{29}$$

F. Collimator

A simplified model of collimator consists of a resistive wall with smaller pipe radius and the steps as well. There are 4 collimator units, each has an overall radius $b_{colli} = 7.5\ cm$, and a length of $\ell_{colli} = 2.43\ m$. Assume the collimators to be made by stainless steel, the same as the vacuum chamber. The collimator resistive wall impedance at ω_0 is,

$$Z_{\ell,wall}(\omega_0) = \frac{4\ell_{colli}}{2\pi R}\frac{b}{b_{colli}} Z_\ell(\omega_0) = 0.04(1+j)\ \Omega \tag{30}$$

and

$$Z_{T,wall}(\omega_0) = \frac{4\ell_{colli}}{2\pi R}\frac{b^3}{b_{colli}^3} Z_T(\omega_0) = 0.52(1+j)\ K\Omega/m \tag{31}$$

The longitudinal and transverse resistive wall impedances are 6% and 10% of the ring impedances, respectively.

For both horizontal and vertical transition impedances, we calculate 8 steps, with $b = 7.5\ cm$, $h = 10\ cm$, i.e.,

$$\frac{Z_\ell}{n} = j1.04\ \Omega \tag{32}$$

and

$$Z_T = j8.3\ K\Omega/m \tag{33}$$

Note that these are much larger than the resistive wall part of impedance.

G. Summary

The total longitudinal broad band impedance is estimated as $Z_\ell/n \approx j17$ Ω.

The broad band impedance is probably the most explored one in the past 3 decades. For instance, in [10,11], it showed to be 14 to 26 Ω for ISR. In [12,13], 20 to 30 Ω for CPS. In [14,15], 10 to 16 Ω for SPS. In [16], it was measured that for AGS, $Z_\ell/n = j30\ \Omega$.

A carefully designed synchrotron nowadays can achieve $Z_\ell/n < j1\ \Omega$. In terms of conventional beam instabilities, however, only moderate tapering and shielding in the transitions are required for the SNS storage ring, given the experience of several low energy proton synchrotrons in operations. For possible elimination of the electron accumulation, which is a possible culprit of the PSR instabilities, smooth chamber transitions might be desired. This issue will be further investigated.

V. Low Frequency Impedance

The low frequency impedance comes mainly from the beam position monitor (BPM), extraction kickers, and injection kickers. The resonant frequency of the low frequency impedance is between several tens to several hundreds MHz, the imaginary part of Z_ℓ/n is less constant in the relevant frequency range, and the real part of the impedance may no longer be negligible.

A. Beam position monitor

Dual plane stripline BPM's will be located adjacent to each quadrupole. One end of the stripline is shorted and another end is terminated for detection.

The longitudinal impedance of one strip plate, for such kind of BPM, is [17,18],

$$Z_\ell = Z_c \left(\frac{\phi_0}{2\pi}\right)^2 \left(\sin^2\frac{\omega\ell}{c} + j\sin\frac{\omega\ell}{c}\cos\frac{\omega\ell}{c}\right) \tag{34}$$

where ℓ and ϕ_0 are the BPM length and subtends, and Z_c is the characteristic impedance of the stripline. One may notice that the lowest resonant frequency of the impedance is at $f_R = c/(4\ell)$. The reactive part, for frequency much smaller than f_R, can be estimated as,

$$\frac{Z_\ell}{n} = j\frac{Z_c}{n}\left(\frac{\phi_0}{2\pi}\right)^2 \sin\frac{\omega\ell}{c}\cos\frac{\omega\ell}{c} \approx jZ_c\left(\frac{\phi_0}{2\pi}\right)^2 \frac{\beta\ell}{R} \tag{35}$$

The transverse impedance can be obtained using the Nassibian-Sacherer derivation from the longitudinal impedance of the displaced beam [19]. For a pair of striplines, it is in the perpendicular direction,

$$Z_T = \frac{R}{\beta b^2}\left(\frac{4}{\phi_0}\right)^2 \sin^2\frac{\phi_0}{2}\left(\frac{Z_\ell}{n}\right) \tag{36}$$

where Z_ℓ is the longitudinal impedance for two striplines. In another direction, it is $Z_T = 0$.

Let ϕ_0 be small, the transverse impedance can be estimated as,

$$Z_T \approx \frac{4R}{\beta b^2}\left(\frac{Z_\ell}{n}\right) \tag{37}$$

In the SNS storage ring, total 40 BPM's are associated with normal quads, where $b = 10\ cm$. Total 8 BPM are associated with large quads, where $b = 15$ cm. All striplines have the length $\ell = 50\ cm$, and the subtends $\phi_0 = 70$ deg. The characteristic impedance of the stripline is $Z_c = 50\ \Omega$.

The longitudinal and transverse impedances are shown in Fig.1.

For the low frequency, $\omega \ll c/\ell$, the longitudinal and transverse impedances can be estimated by (35) and (37). Thus, for 48 pairs of plates, we have,

$$\frac{Z_\ell}{n} \approx j2.58\ \Omega \tag{38}$$

and,

$$Z_T \approx j41.4\ k\Omega/m \tag{39}$$

Note that these are a little different from that shown in Fig.1.

B. Extraction kickers

1. Transverse impedance

In a window frame magnet, the transverse impedance is dominated by the differential flux in the core induced by the beam position deviation. Differential flux generated by the beam is the same as two parallel wires, one represents the beam, and another returned at the position center, terminated

at both ends. Neglecting the chamber effect, the conductor shielding effect, the ferrite boundary effects, etc. this yields the transverse impedance [19]

$$Z_T = \frac{c\omega\mu_0^2\ell^2}{4a^2 Z_k} \ \Omega/m \tag{40}$$

where ℓ is the magnet length, $2a$ is the inner height, and $Z_k = j\omega L + Z_g$, with L the magnet inductance, and Z_g the termination impedance. Results of measurement performed on several kickers are in agreement with this formulation [19,20].

The SNS extraction kicker has 8 window frame magnet units, the average length is $\ell = 40\ cm$, and the average inner width is $2b = 14\ cm$, all have the same height $2a = 11.5\ cm$.

The magnet inductance of each unit is $L = \mu_0 b\ell/a = 0.61\ \mu H$. The stray inductance is about $L_{stray} = 0.5\ \mu H$. For the simplified model with only the charging resistor $R_{ch} = 200\ \Omega$ as the winding termination, the impedance is shown in Fig.2.

We note, however, more realistic magnet winding termination gives rise to very different impedance. Between the magnet and the charging circuits there is a PFN, consisted of 20 sections, with $L_{pfn} = 0.15\ \mu H$, and $C_{pfn} = 4.15\ nF$, terminated by a 6 Ω resistor. Placing two stray capacitance of 50 pf around the stray inductance, the equivalent circuit and the corresponding transverse impedance are shown in Fig.3.

The sensitivity of the impedance with respect to the terminations are demonstrated in Fig.4, where the only variable is the charging resistance. The impedance varies largely.

We note that in a travelling wave kicker, the energy propagation speed is low, and the low frequency impedance is dominated [21,22], which is less sensitive with respect to the terminations.

2. Longitudinal impedance

Consider the beam passes a ferrite ring with the outer and inner radii b_2 and b_1. The inductance of the ferrite ring is

$$L = \frac{\mu_r\mu_0\ell}{2\pi} \ln\frac{b_2}{b_1} \tag{41}$$

where μ_r is the relative permeability. For CMD5005 used in the extraction kicker, $\mu_r \approx 1000$. Taking the equivalent $b_2 = 8.8\ cm$, and $b_1 = 6.3\ cm$ for the extraction kicker magnet, we get $L = 26.7\ \mu H$ for each module.

To reduce the massive ferrite loss, copper sheets are placed in the ferrite core as flux break.

Let the thickness of the copper sheet be δ_{copper}, then the corresponding leakage is estimated as [23],

$$L_{leak} = 2\frac{\mu_0 \ell}{2\pi} \ln \frac{\pi a}{2\delta_{copper}} \tag{42}$$

Taking $\delta_{copper} = 1\ mm$, $2a = 11.5\ cm$, we get $L_{leak} = 0.72\ \mu H$ for $\ell = 40\ cm$, i.e. one magnet module. This is 2.7% of the flux generated without the copper sheet. The leakage of approximately $3\% \sim 4\%$ is obtained by a simulation, shown in Fig.5 [24]. The shielding effect of the copper conductor is under study. If we take a 1% flux leakage around the copper sheet, the total inductance of 8 modules presented to the beam is $L_m = 2.14\ \mu H$. Using

$$\frac{Z_\ell}{n} = j\omega_0 L_m \tag{43}$$

we get the equivalent longitudinal impedance of $Z_\ell/n = j\ 16\ \Omega$.

We note that the beam image current at the conductor, which is used as the magnet winding, will partly offset the field created by the beam, therefore, the flux induced in the core should be lower. This reduction will be estimated in the measurement.

On the other hand, the Nassibian-Sacherer approach has a longitudinal impedance

$$Z_\ell = \frac{\omega^2 \mu_0^2 x_0^2 \ell^2}{4a^2 Z_k} \Omega \tag{44}$$

with x_0 the position shift. For $x_0 = 1\ cm$, $|Z/n|$ is in $\sim$0.1 Ω range, which is negligible compared with the flux leakage.

It is interesting to note that the SNS longitudinal space charge impedance is $-j\ 196\ \Omega$, which is negative inductive. Therefore, the magnet flux leakage may compensate a part of that impedance.

Compensation of the longitudinal space charge impedance has been studied by inserting ferrite rings in the beam pipe, such as that at PSR [25] and KEK PS [26]. This approach is also proposed for the muon-collider proton

driver [27]. If handled carefully, the ferrite window frame used for the extraction kicker may be used for the same purpose. A thinner copper sheet might be used without causing a heating problem [28], which is associated with the real part of the impedance.

Finally, a complete model will include a differential flux leakage through the gap air, L_ℓ. Assuming $L_\ell = L_m/2$, and let the parasitic capacitance be 50 pf, the longitudinal impedance is shown in Fig.6 and Z_ℓ/n in Fig.7. Termination is again very important [29,30].

C. Injection kickers

There are 4 units of horizontal and 4 units of vertical kickers, all have same window frame magnet, with copper sheets inserted. The inner height and width are $2b = 2a = 16\ cm$, with the length $\ell = 34\ cm$. The injection kickers are desired to have a response time constant of $\tau = 150\ \mu s$, to accommodate horizontal and vertical painting. To reduce the impedance, it is preferred to put the kicker magnet outside of the vacuum chamber. The rise time due to the shielding by eddy current is [31,32],

$$\tau_{rise} = \frac{\mu_0 \sigma b d_{cond}}{2} \tag{45}$$

where b is the vacuum chamber radius, d_{cond} is the thickness of the chamber conductor, and $\sigma = 1/\rho = 1.37 \times 10^6\ (\Omega m)^{-1}$ is the conductivity for stainless steel.

A 0.03" inconel wall is presently under consideration. With $d_{cond} = 0.76$ mm and $\sigma = 10^6\ (\Omega m)^{-1}$, we get $\tau_{rise} = 38\ \mu s$. The desired injection kicker dynamics with $\tau = 150\ \mu s$ and the response with this wall are shown in Fig. 8.

1. Transverse impedance

Different from the extraction kicker, these injection kickers have 10 turns of windings. Therefore, the termination impedance seen by the beam is reduced to about 1%, and the termination becomes much less sensitive, compared with the extraction kickers.

Only the beam frequency below the skin depth frequency f_{skin} can penetrate the wall [32], with

$$f_{skin} = \frac{1}{\pi \mu_0 \sigma d_{cond}^2} \tag{46}$$

then the cutoff frequency is $f_{skin} = 0.45\ MHz$ for the 0.03" inconel wall. The resulted impedance is negligible compared with the extraction kickers.

2. Longitudinal impedance

The longitudinal impedance is also calculated similarly to the one for extraction kickers, except that a resistance of the wall is in parallel with the mutual inductance shown in Fig.6. For the 0.03" inconel wall, the resistance is $R = \rho \ell / (2\pi b d_{cond}) = 0.9\ m\Omega$. Therefore, the longitudinal impedance and the heating are both negligible.

VI. Narrow Band Impedance

For the fundamental mode of the RF cavities, the impedance can be expressed as

$$Z = \frac{R_{sh}}{1 + jQ(\omega/\omega_R - \omega_R/\omega)} \tag{47}$$

where R_{sh} and Q are the shunt resistance and quality factor of the loaded cavity, respectively, and ω_R is the resonant frequency.

There are 3 RF stations in the ring, each station consists of 2 gaps, at 6.7 KV per gap [33]. The second harmonic consists of 1 station, with 2 gaps at 10 KV per gap. The same ferrite of the AGS Booster band III cavities, Phillips 4M2, will be used. The design of $h = 1$ and $h = 2$ cavities is the same.

The relative permeability is $\mu_r = 130$ for Phillips 4M2. Taking the ferrite length $\ell = 80\ cm$, the inner radius $r_{in} = 12\ cm$, and the outer radius $r_{out} = 24.5\ cm$, the total inductance of a gap is

$$L = \frac{\mu_r \mu_0 \ell}{2\pi} \ln \frac{r_{out}}{r_{in}} = 14.8\ \mu H \tag{48}$$

The inherent capacitance is

$$C_{inh} = \frac{2\pi \epsilon_0 \ell}{\ln(r_{out}/r_{in})} \tag{49}$$

where $\epsilon_0 = 1/(\mu_0 c^2) = 8.8542 \times 10^{-12}\ F/m$. We get $C_{inh} = 62.4\ pF$.

The capacitance needed to get $\omega_R = 2\pi \times 1.189\ MHz$ is $C_1 = 1.2\ nF$ for $h = 1$ cavities, and $C_2 = 0.3\ nF$ for $h = 2$ cavities. The inherent capacitance is small compared with the added ones.

The ferrite resistance is $R_{ferr} = 10\ K\Omega$ per gap, and the generator resistance is $R_{gen} = 375\ \Omega$. Therefore, we have the shunt resistance of a gap,

$$R_{sh} \approx R_{gen} = 375\Omega \tag{50}$$

The loaded cavity quality factor is

$$Q_1 = R_{sh}\sqrt{\frac{C_1}{L}} = 3.38 \tag{51}$$

For $h = 2$ cavity, it is $Q_2 = 1.69$.

The longitudinal high order modes and the transverse modes will be estimated using simulation codes. Once a prototype of cavities becomes available, measurement will be performed.

The possible narrow band impedance caused by large steps and cavities in the vacuum chamber will also be studied by the simulations.

VII. Acknowledgment

I would like to thank H.C. Hseuh, A. Soukas, M. Blaskiewicz, M. Mapes, J.G. Wang, Y.Y. Lee, W.T. Weng, J. Touzzolo, R. Witkover, T. Shea, H. Ludewig, J. Wei, and W. Meng, for valuable discussions.

References

[1]A. Chao, *Physics of Collective Beam Instabilities in High Energy Accelerators*, Wiley, New York, 1994.

[2]F. Ruggiero, Particle Accelerators, Vol.50, p.83, 1995.

[3]S.Y. Zhang, SNS Tech. Note, No.33, April 1997.

[4]Y.Y. Lee, NSNS Tech. Notes, No.26, BNL, Feb. 1997.

[5]S.S. Kurennoy and G.V. Stupakov, Particle Accelerators, Vol.45, p.95, 1994.

[6]K. Bane, SLAC-PUB-4618, May 1988.

[7]S.S. Kurennoy, Particle Accelerators, Vol.39, p.1, 1992.

[8]M. D'yachkov and F. Ruggiero, LHC Project Report, 104, 1997.

[9]M. Blaskiewicz, SNS Tech. Note, No.46, Aug. 1998.

[10]P. Bramham et. al. IEEE Trans. NS, Vol.NS-24, No.3, p.1490, 1977.

[11]S. Hansen et. al. IEEE Trans. NS, Vol.NS-22, No.3, p.1381, 1975.

[12]J. Gareyte, PS/DL/Note 76-10, CERN, 1976.

[13]D. Boussard et. al. PS OP/LR Note 80-16, CERN, 1980.

[14]D. Boussard and J. Gareyte, SPS/AC/DB/JG/EEK, Improvement Report No.181, CERN 1980.

[15]T. Linnecar and E. Shaposhnikova, CERN-SL-96-45, RF, July, 1996.

[16]F. Pedersen and E. Raka, IEEE Trans. NS, Vol.NS-26,No.3, p.3592, 1979.

[17]R.E. Shafer, IEEE Trans. NS, Vol.NS-32,No.5, p.1933, 1985.

[18]K.Y. Ng, Particle Accelerators, Vol.23, p.93, 1988.

[19]G. Nassibian and F. Sacherer, Nucl. Inst. Meth. Vol.159, p21, 1979.

[20]U. Blell, p.1727, PAC 1997.

[21]G. Lambertson and K.Y. Ng, Workshop on RHIC Performance, March, 1988.

[22]K.Y. Ng, AIP Conference Proceedings, 184, 1989.

[23]G. Lambertson, Workshop on RHIC Performance, March, 1988.

[24]W.Z. Meng, private communication.

[25]J. Griffin et. al., FN-661, 1997.

[26]K. Koba, et. al., KEK Preprint 97-173, 1997.

[27]K.Y. Ng, Fermilab-FN-659, July7, 1997.

[28]W.K. vanAsselt and Y.Y. Lee, PAC91, p.881, 1991.

[29]F. Voelker and G. Lambertson, p.851, PAC 1989.

[30]A. Ratti and T.J. Shea, p.1803, PAC 1991.

[31]S.S. Kurennoy, p.3417, PAC 1993.

[32]S. Peggs and W.W. MacKay, RHIC/AP/36, Sep. 1994.

[33]M. Blaskiewicz, J.M. Brennan, and A. Zaltsman, SNS Tech. Note, No.36, May, 1997.

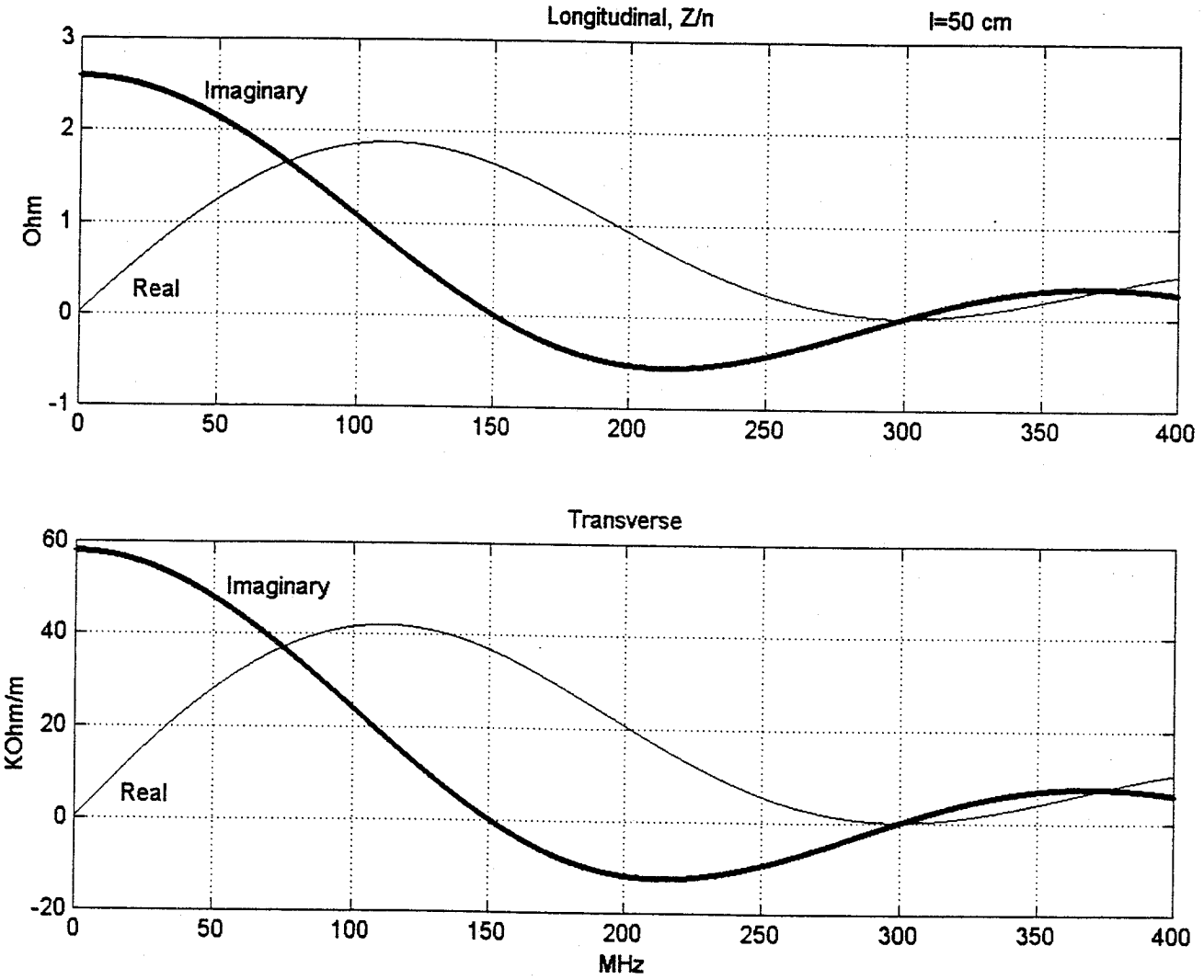

Fig.1. *BPM Impedance*

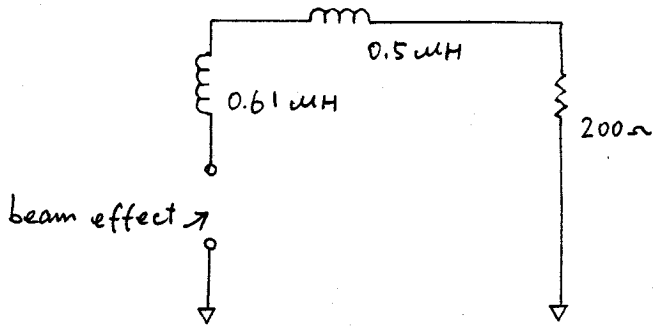

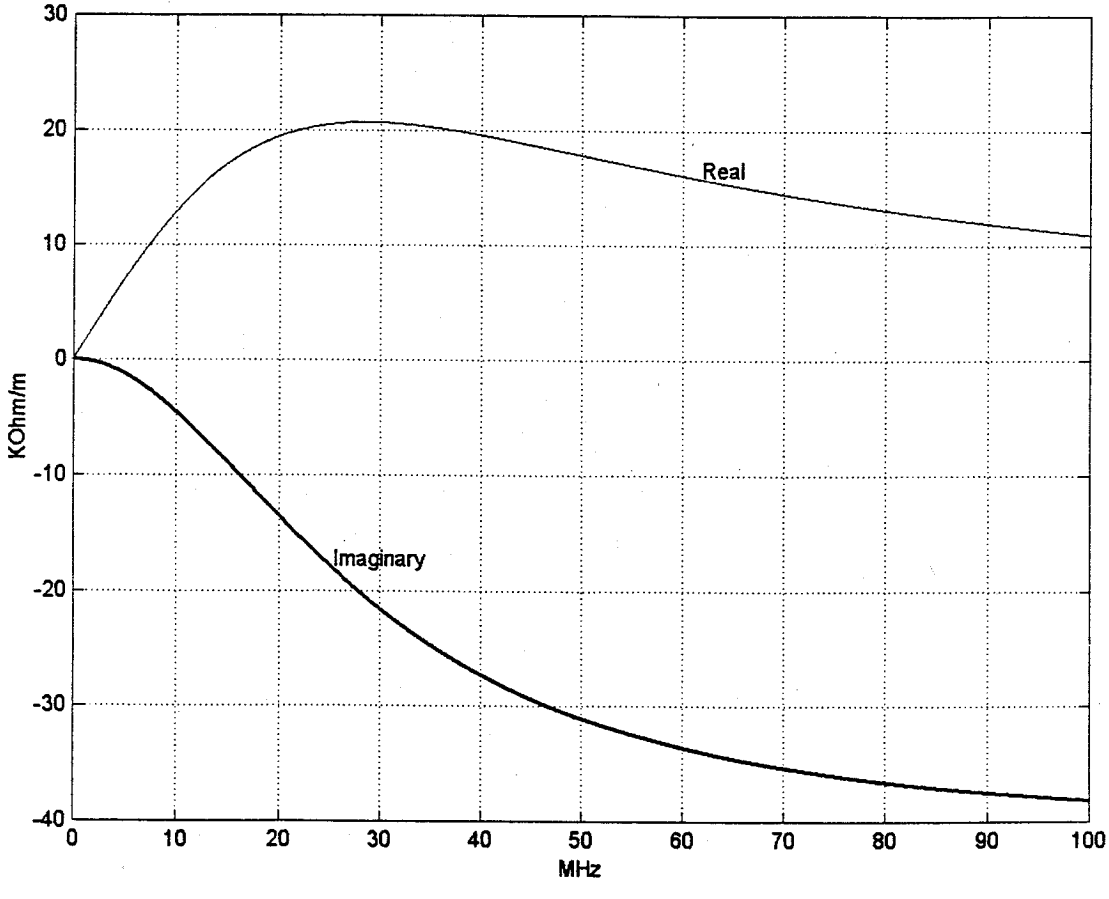

Fig.2. *Simplified Equivalent Circuit and Impedance of Extraction Kickers, Transverse*

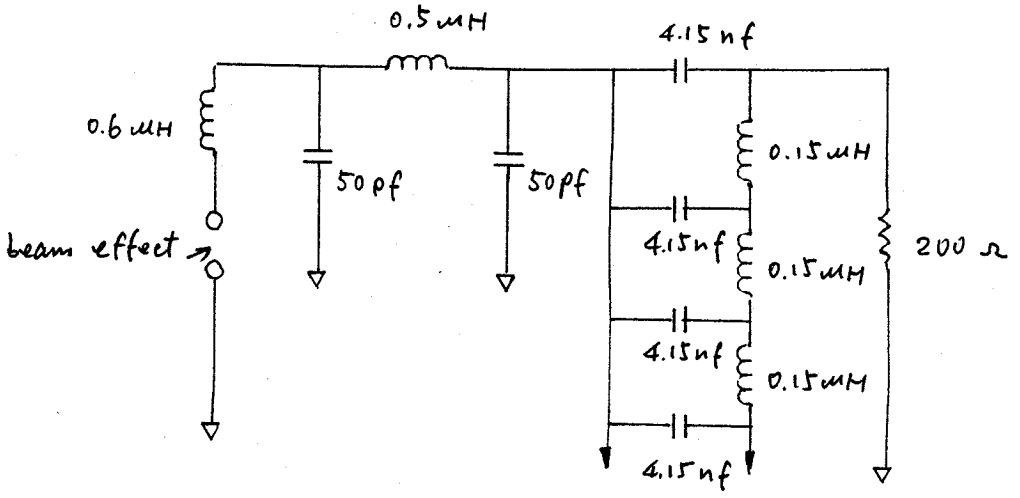

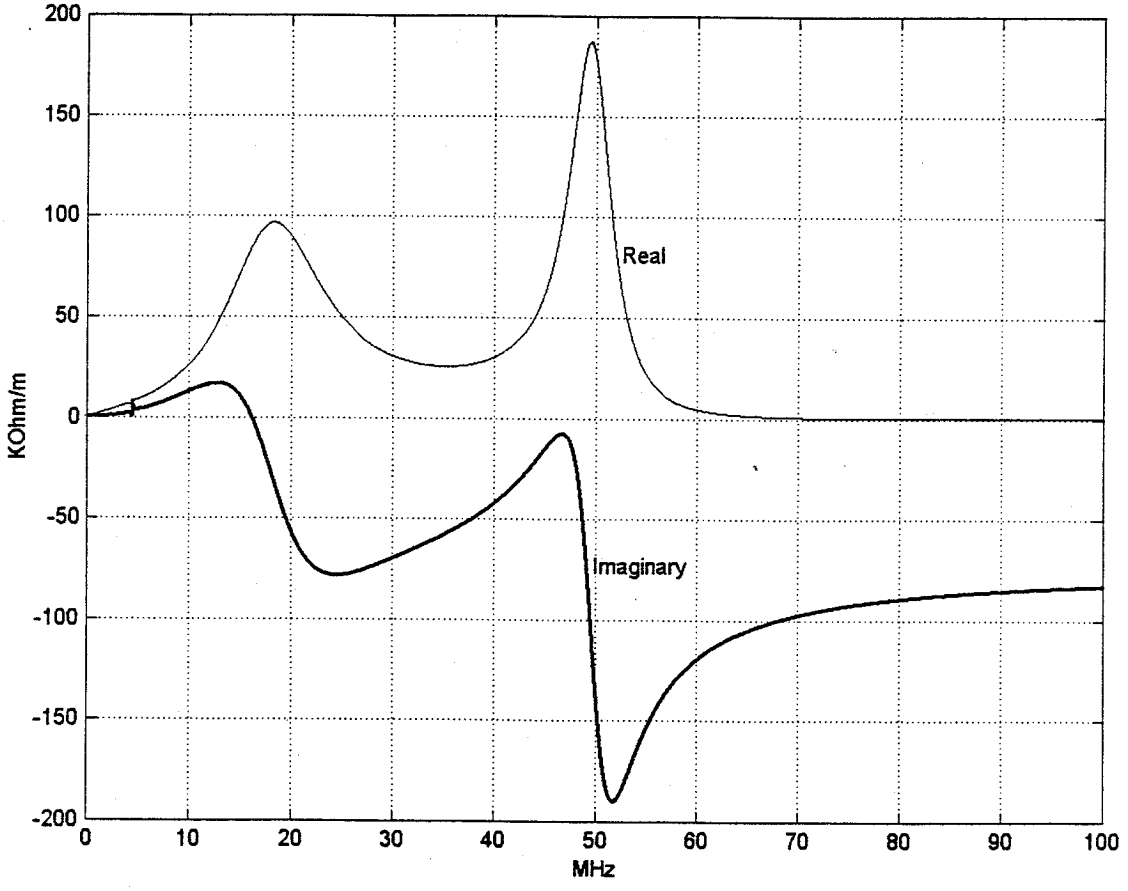

Fig.3. *More Realistic Equivalent Circuit and Impedance of Extraction Kickers, Transverse*

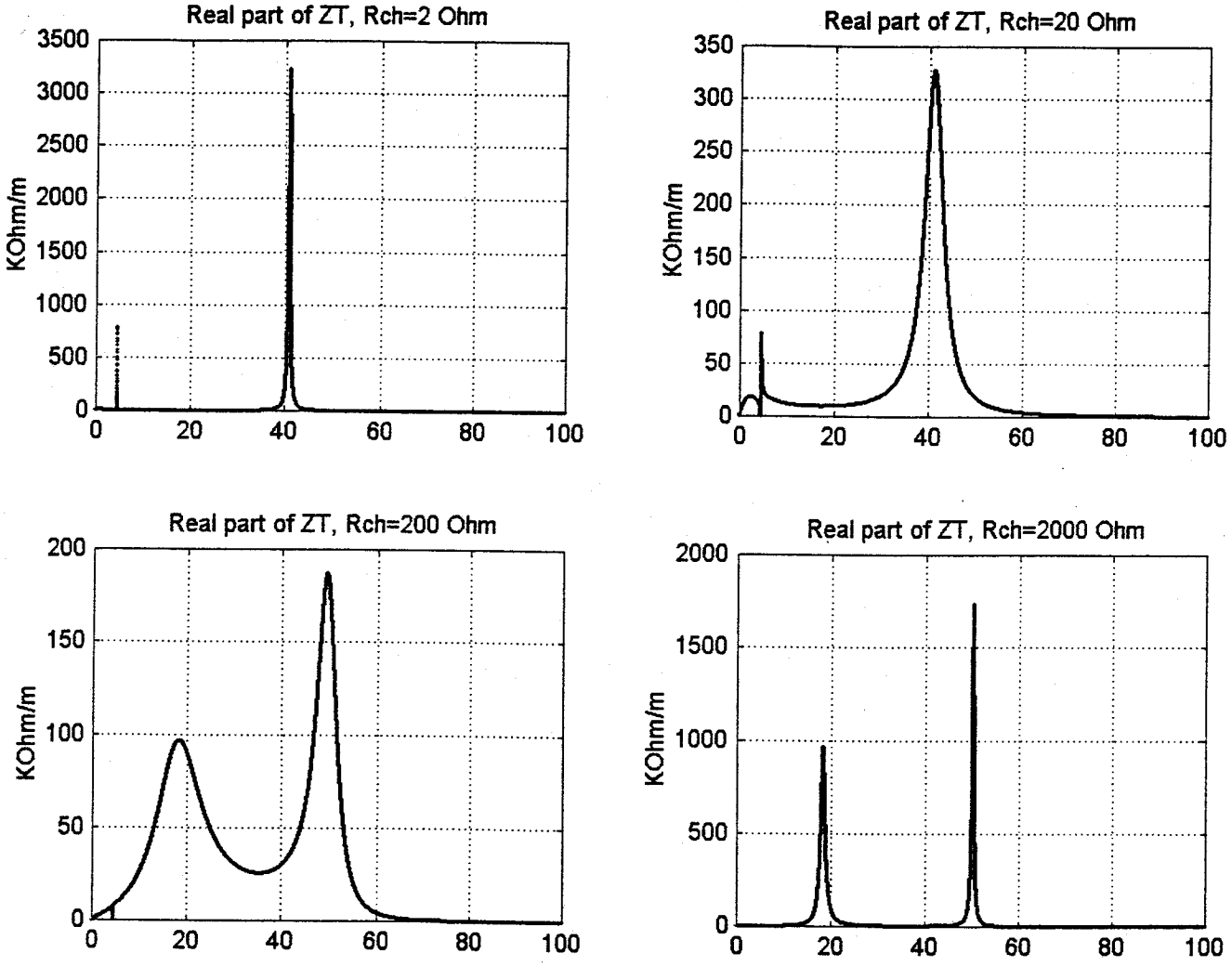

Fig.4. *Sensitivity of Extraction Kickers Impedance w.r.t. Terminations, Transverse*

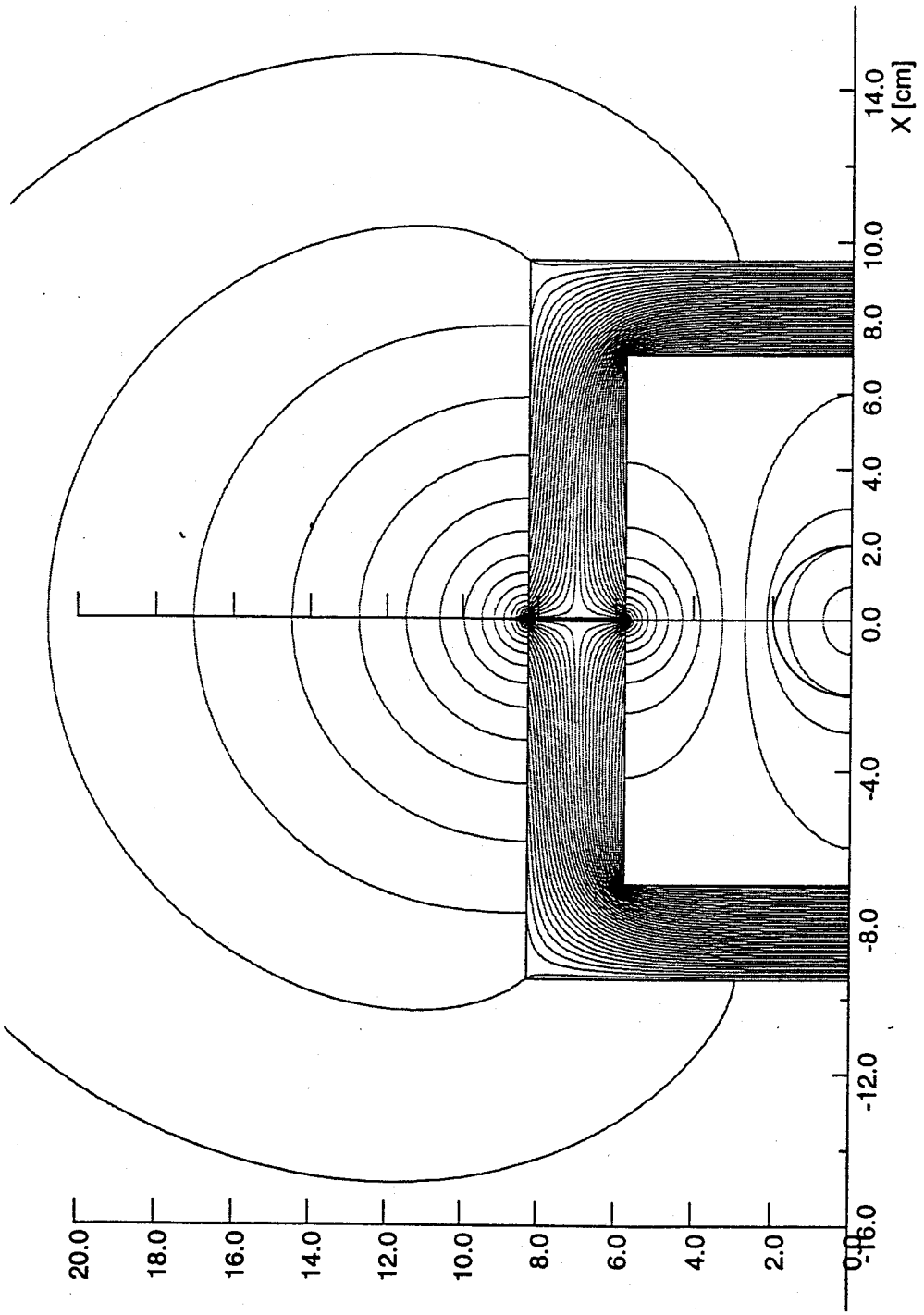

Fig.5. *Flux Leakage in Extraction Kicker magnet*

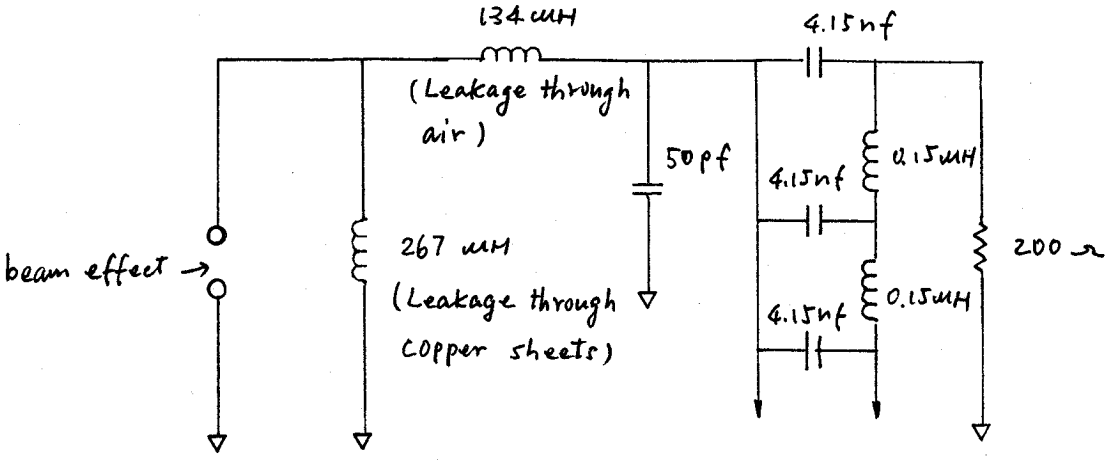

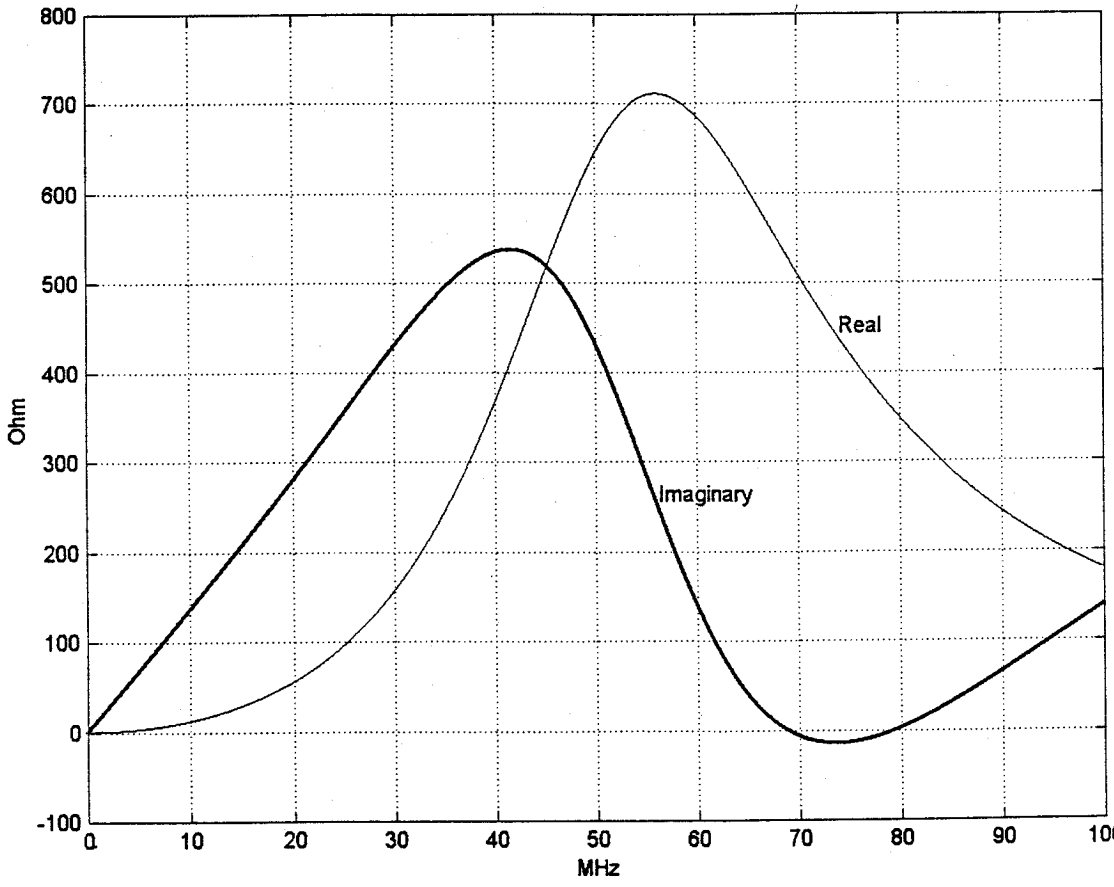

Fig.6. *Equivalent Circuit and Impedance of Extraction Kickers, Longitudinal*

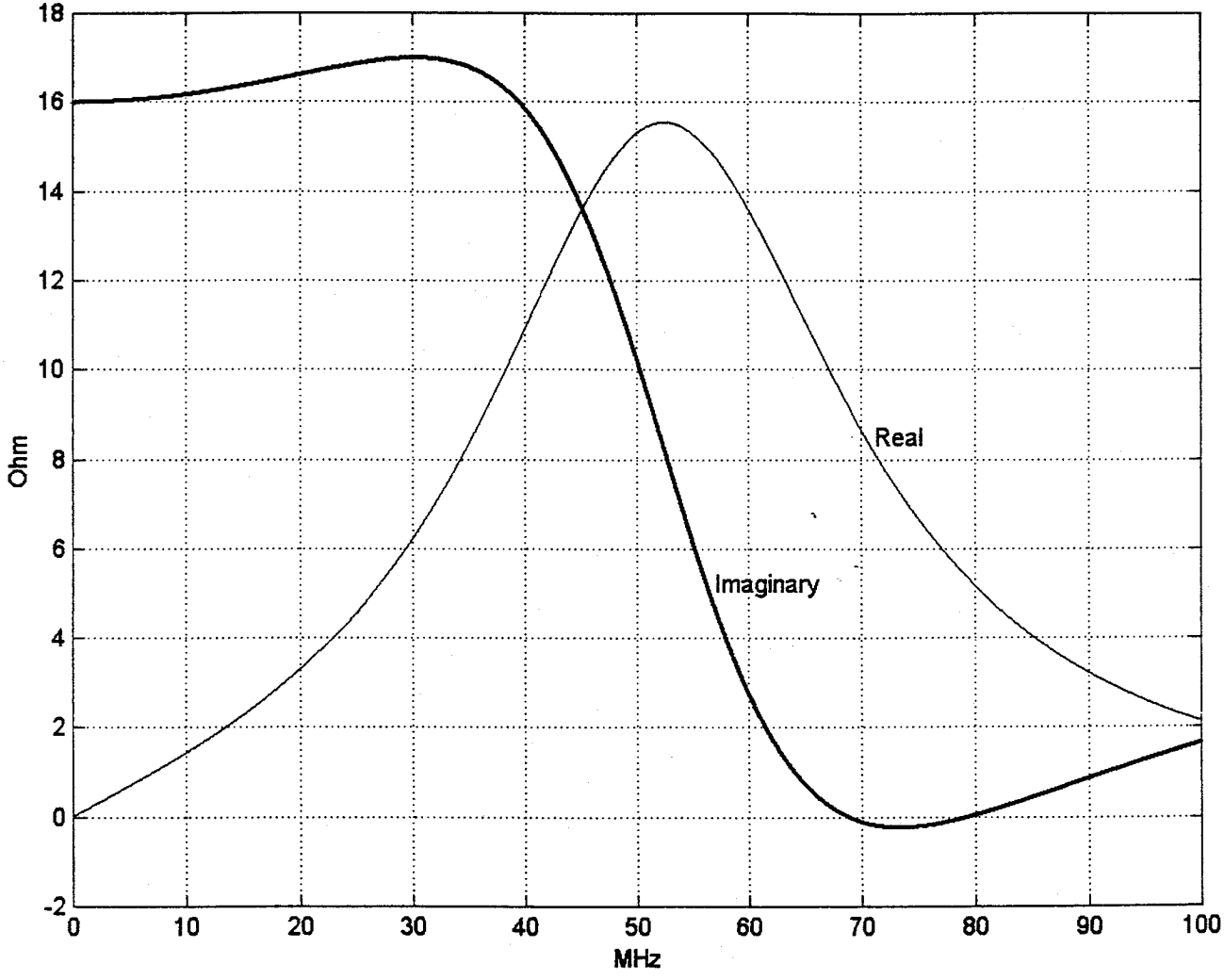

Fig.7. *Impedance of Extraction Kickers, Longitudinal, Z/n*

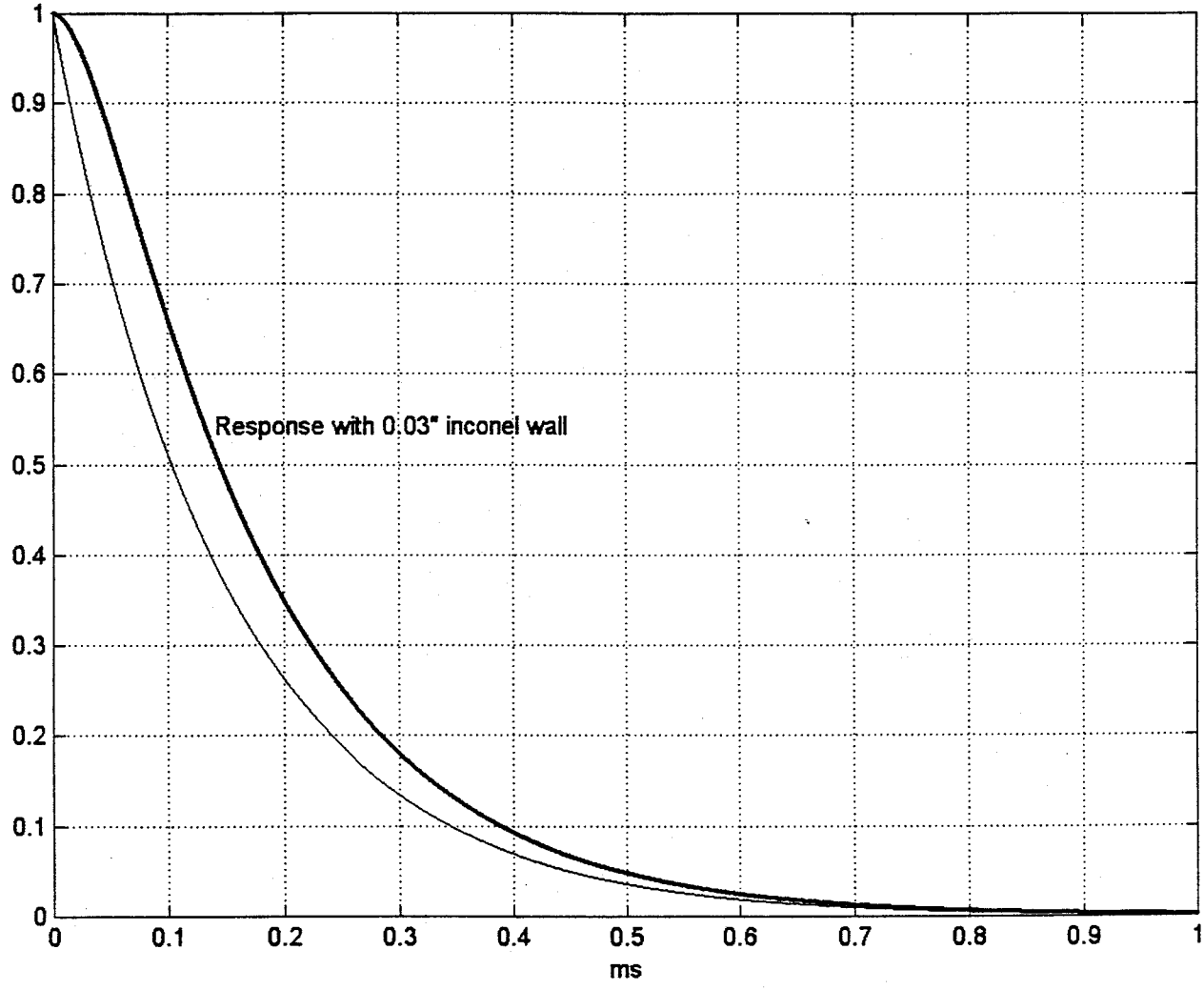

Fig.8. *Response of Injection Kickers*